Supporting Information

Nanothermometers based on lanthanide incorporated Periodic Mesoporous Organosilica

Anna M. Kaczmarek*, Rik Van Deun, Pascal Van Der Voort*

Table S1. Relative Ln^{3+} contents for the Eu_xTb_yDPA-PMO and Sm_xTb_yDPA-PMO samples during synthesis (calcd.) and as determined by XRF.

Sample	Molar amounts used in synthesis [mmol]			Eu^{3+} ion		Sm^{3+} ion		Tb^{3+} ion	
	$EuCl_3$	$SmCl_3$	$TbCl_3$	Calcd.	XRF	Calcd.	XRF	Calcd.	XRF
$Eu_{0.25}Tb_{0.75}$DPA-PMO	0.25	-	0.75	25%	23.4%	-	-	75%	76.6%
$Eu_{0.50}Tb_{0.50}$DPA-PMO	0.50	-	0.50	50%	46.1%	-	-	50%	53.9%
$Eu_{0.75}Tb_{0.25}$DPA-PMO	0.75	-	0.25	75%	74.7%	-	-	25%	25.3%
$Sm_{0.90}Tb_{0.10}$DPA-PMO	-	0.90	0.10	-	-	90%	87.7%	10%	12.3%
$Sm_{0.95}Tb_{0.05}$DPA-PMO	-	0.95	0.05	-	-	95%	95.8%	5%	4.2%

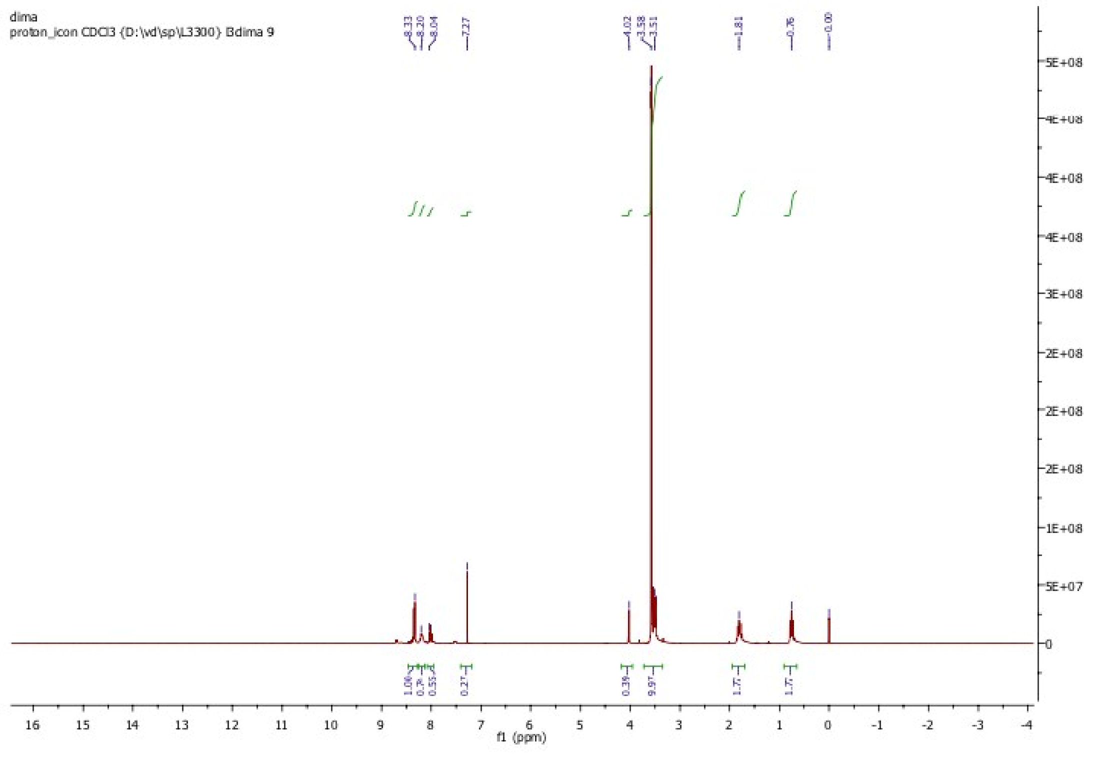

Fig. S1 ^{1}H NMR of the DPA-PMO precursor ($CDCl_3$, 300 MHz).

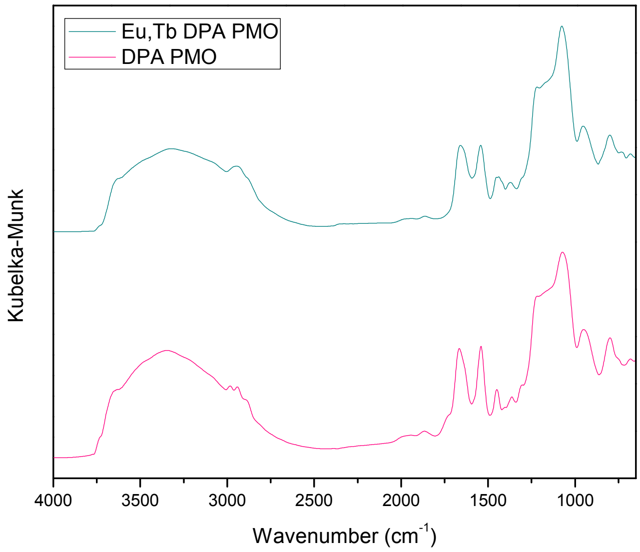

Fig. S2 FT-IR spectra of DPA-PMO and $Eu_{0.50}Tb_{0.50}$DPA-PMO.

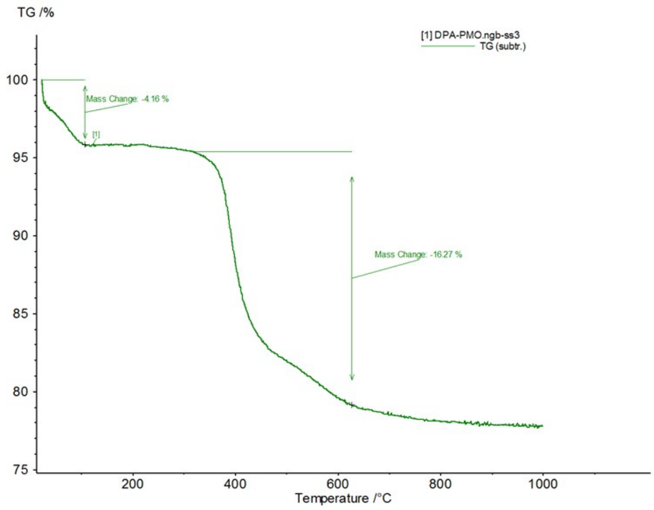

Fig. S3 TG analysis of DPA-PMO material.

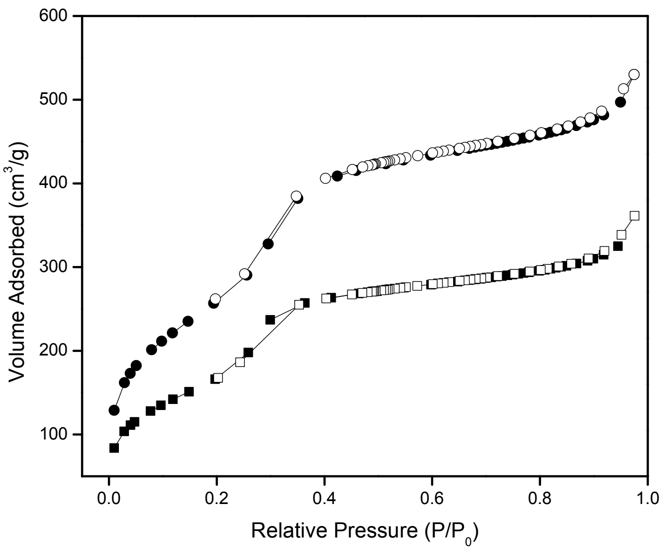

Fig. S4 N_2 adsorption-desorption isotherm of DPA-PMO (circles) and $Eu_{0.25}Tb_{0.75}$DPA-PMO (squares).

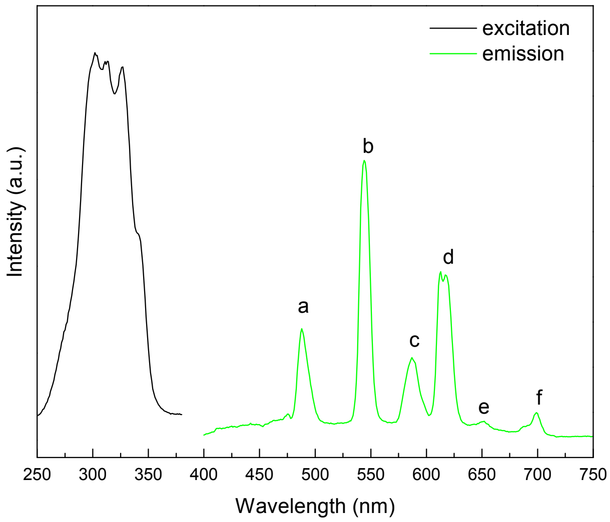

Fig. S5 Room temperature combined excitation-emission spectrum of sample $Eu_{0.25}Tb_{0.75}$DPA-PMO (excited a 326.0 nm and observed at 544.6 nm).

Table S2 Assignment of peaks labeled in Fig. S5 ($Eu_{0.25}Tb_{0.75}$DPA-PMO).

Peak	Wavelength (nm)	Wavenumber (cm^{-1})	Transition
		Emission	
a	488.5	20470	$^5D_4 \rightarrow {}^7F_6$ (Tb)
b	544.6	18362	$^5D_4 \rightarrow {}^7F_5$ (Tb)
c	587.5	17021	$^5D_0 \rightarrow {}^7F_1$ (Eu)
d	613.0	16313	$^5D_0 \rightarrow {}^7F_2$ (Eu)
e	650.8	15365	$^5D_0 \rightarrow {}^7F_3$ (Eu)
f	699.7	14292	$^5D_0 \rightarrow {}^7F_4$ (Eu)

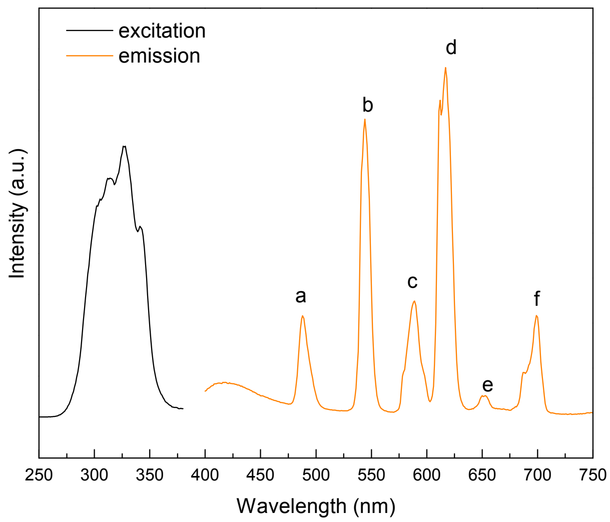

Fig. S6 Room temperature combined excitation-emission spectrum of sample $Eu_{0.50}Tb_{0.50}$DPA-PMO (excited a 326.0 nm and observed at 617.1 nm).

Table S3. Assignment of peaks labeled in Fig. S6 ($Eu_{0.50}Tb_{0.50}$DPA-PMO).

Peak	Wavelength (nm)	Wavenumber (cm^{-1})	Transition
		Emission	
a	487.4	20517	$^5D_4 \rightarrow {}^7F_6$ (Tb)
b	544.6	18362	$^5D_4 \rightarrow {}^7F_5$ (Tb)
c	588.5	16992	$^5D_0 \rightarrow {}^7F_1$ (Eu)
d	617.1	16205	$^5D_0 \rightarrow {}^7F_2$ (Eu)
e	651.8	15342	$^5D_0 \rightarrow {}^7F_3$ (Eu)
f	699.4	14298	$^5D_0 \rightarrow {}^7F_4$ (Eu)

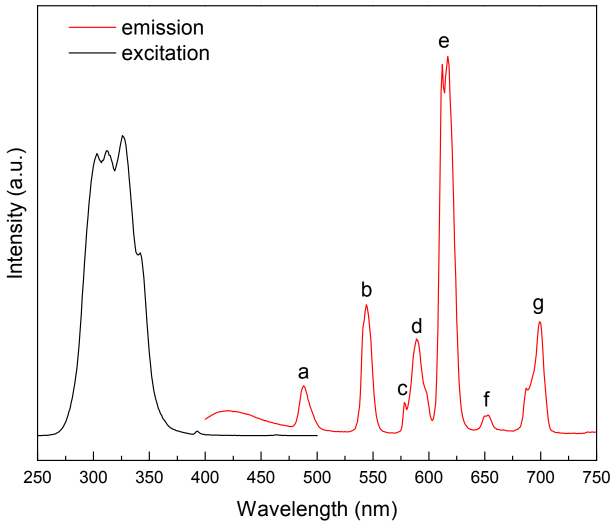

Fig. S7 Room temperature combined excitation-emission spectrum of sample $Eu_{0.75}Tb_{0.25}$DPA-PMO (excited a 326.0 nm and observed at 617.7 nm).

Table S4. Assignment of peaks labeled in Fig. S7 ($Eu_{0.75}Tb_{0.25}$DPA-PMO).

Peak	Wavelength (nm)	Wavenumber (cm^{-1})	Transition
		Emission	
a	488.1	20487	$^5D_4 \rightarrow {}^7F_6$ (Tb)
b	544.0	18382	$^5D_4 \rightarrow {}^7F_5$ (Tb)
c	579.3	17262	$^5D_0 \rightarrow {}^7F_0$ (Eu)
c	589.8	16955	$^5D_0 \rightarrow {}^7F_1$ (Eu)
d	617.7	16189	$^5D_0 \rightarrow {}^7F_2$ (Eu)
e	651.5	15349	$^5D_0 \rightarrow {}^7F_3$ (Eu)
f	698.9	14308	$^5D_0 \rightarrow {}^7F_4$ (Eu)

Table S5. CIE color coordinates (x, y) at different temperatures for $Eu_{0.25}Tb_{0.75}$DPA-PMO.

Temperature [K]	x coordinate	y coordinate
260	0.4081	0.4864
280	0.4042	0.4855
300	0.4066	0.4824
320	0.4124	0.4773
340	0.4221	0.4589
360	0.4323	0.4580
380	0.4509	0.4413
400	0.4586	0.4334

420	0.4677	0.4218
440	0.4810	0.4051
460	0.4964	0.3898

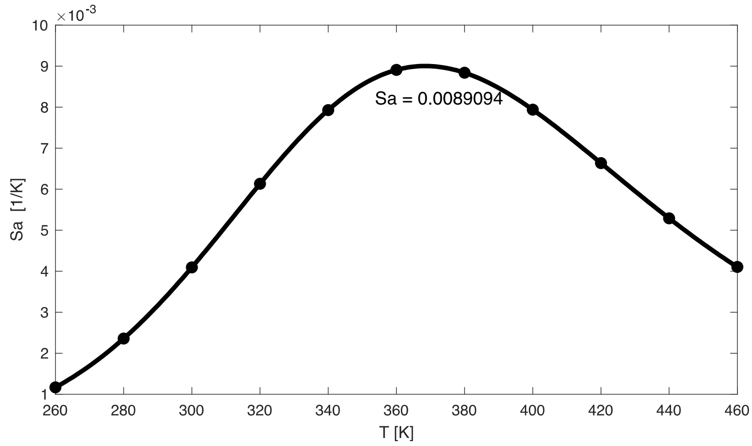

Fig. S8 Plot presenting the absolute sensitivity Sa values at varied temperatures (260K – 460K) for $Eu_{0.25}Tb_{0.75}$DPA-PMO.The solid lines are guides for eyes.

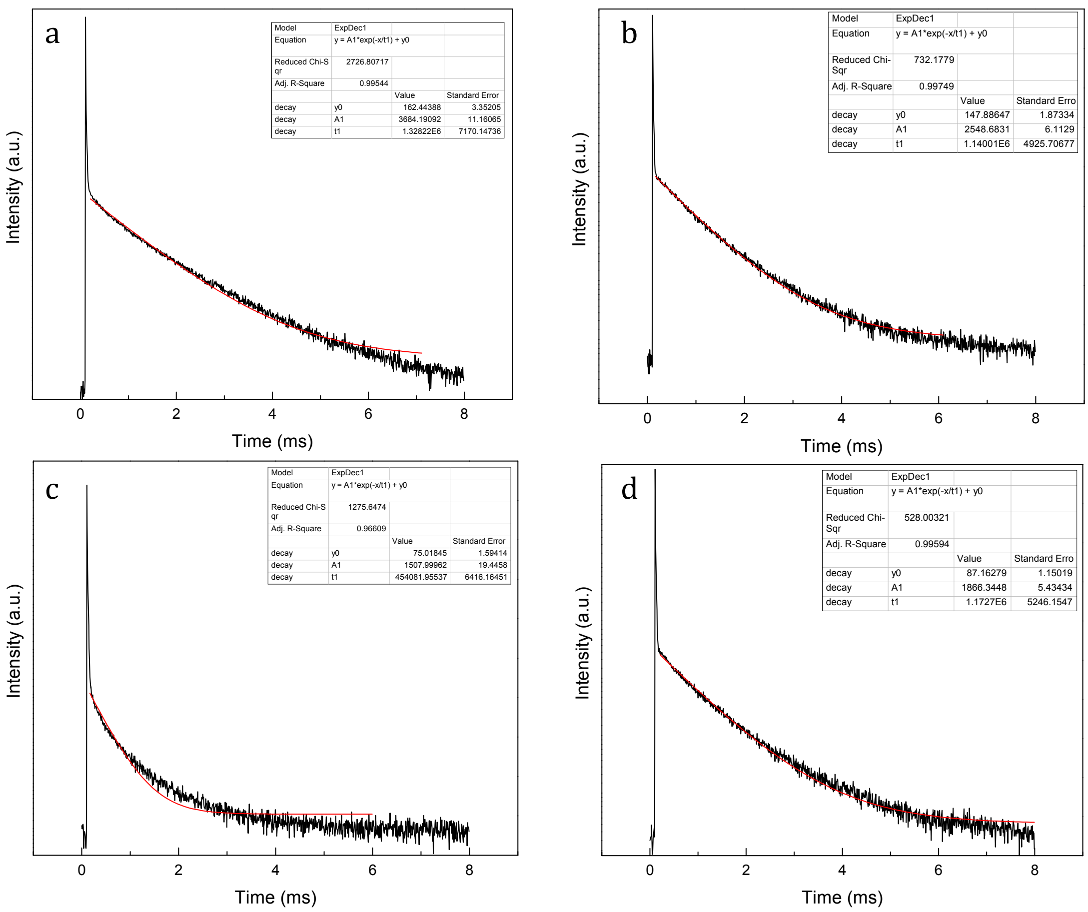

Fig. S9 Decay profiles for sample $Eu_{0.25}Tb_{0.75}$DPA-PMO a) 260 K observed at 544.6 nm (Tb), b) 260 K observed at 613.0 nm (Eu), c) 460 K observed at 544.6 nm (Tb), d) 460K observed at 613.0 nm (Eu). All decay times were recorded when exciting at 326.0 nm.

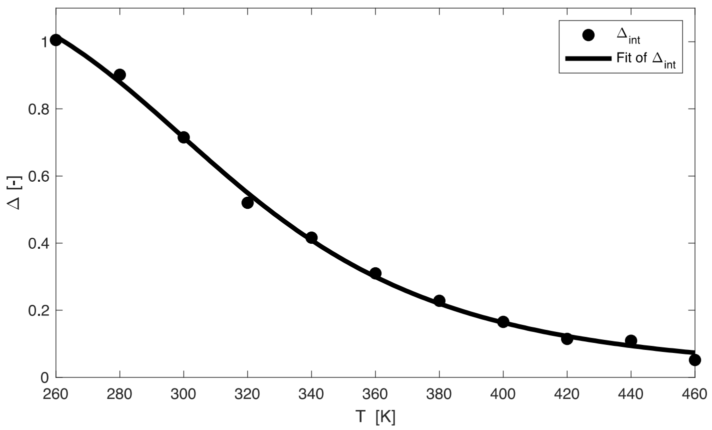

Fig. S10 Plot presenting the calibration curve for $Eu_{0.50}Tb_{0.50}$DPA-PMO material when eqn (2) is employed. The points show the experimental delta parameters and the solid line shows the best fit of the experimental points using eqn (2) (R^2 = 0.99778).

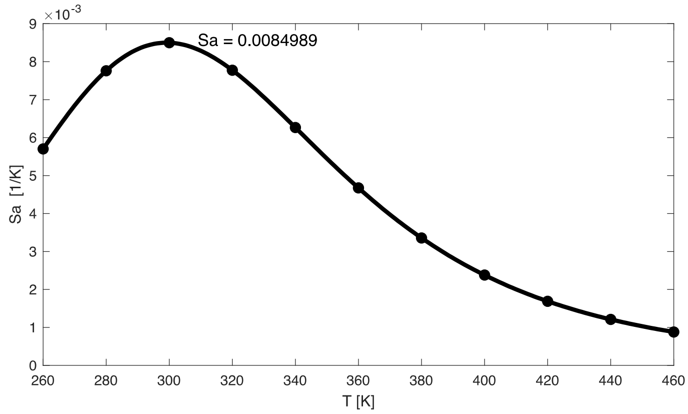

Fig. S11 Plot presenting the absolute sensitivity Sa values at varied temperatures (260K – 460K) for $Eu_{0.50}Tb_{0.50}$DPA-PMO.The solid lines are guides for eyes.

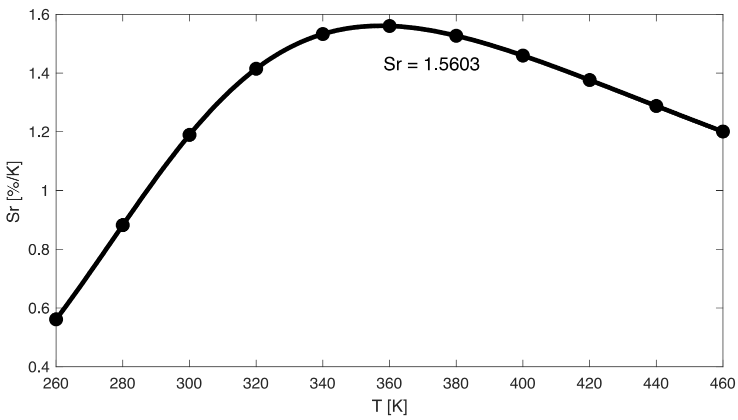

Fig. S12 Plot presenting the relative sensitivity Sr values at varied temperatures (260K – 460K) for compound $Eu_{0.50}Tb_{0.50}$DPA-PMO. The solid lines are guides for eyes.

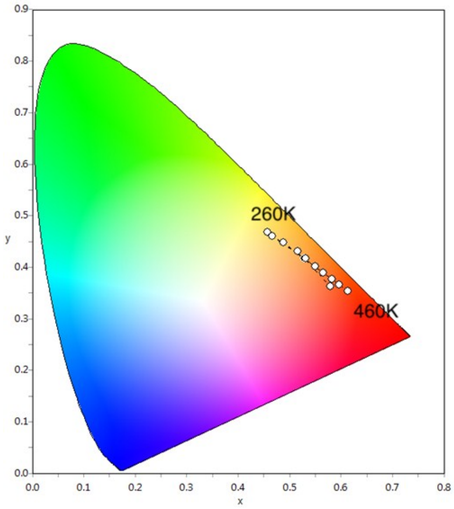

Fig. S13 CIE coordination diagram where the change of color for the $Eu_{0.50}Tb_{0.50}$DPA-PMO material is shown from 260 K to 460 K.

Table S6. CIE color coordinates (x, y) at different temperatures for $Eu_{0.50}Tb_{0.50}$DPA-PMO.

Temperature [K]	x coordinate	y coordinate
260	0.4566	0.4676
280	0.4663	0.4608
300	0.4879	0.4472
320	0.5155	0.4300
340	0.5313	0.4169
360	0.5503	0.4017
380	0.5660	0.3896
400	0.5833	0.3765
420	0.5964	0.3663
440	0.5788	0.3632
460	0.6133	0.3526

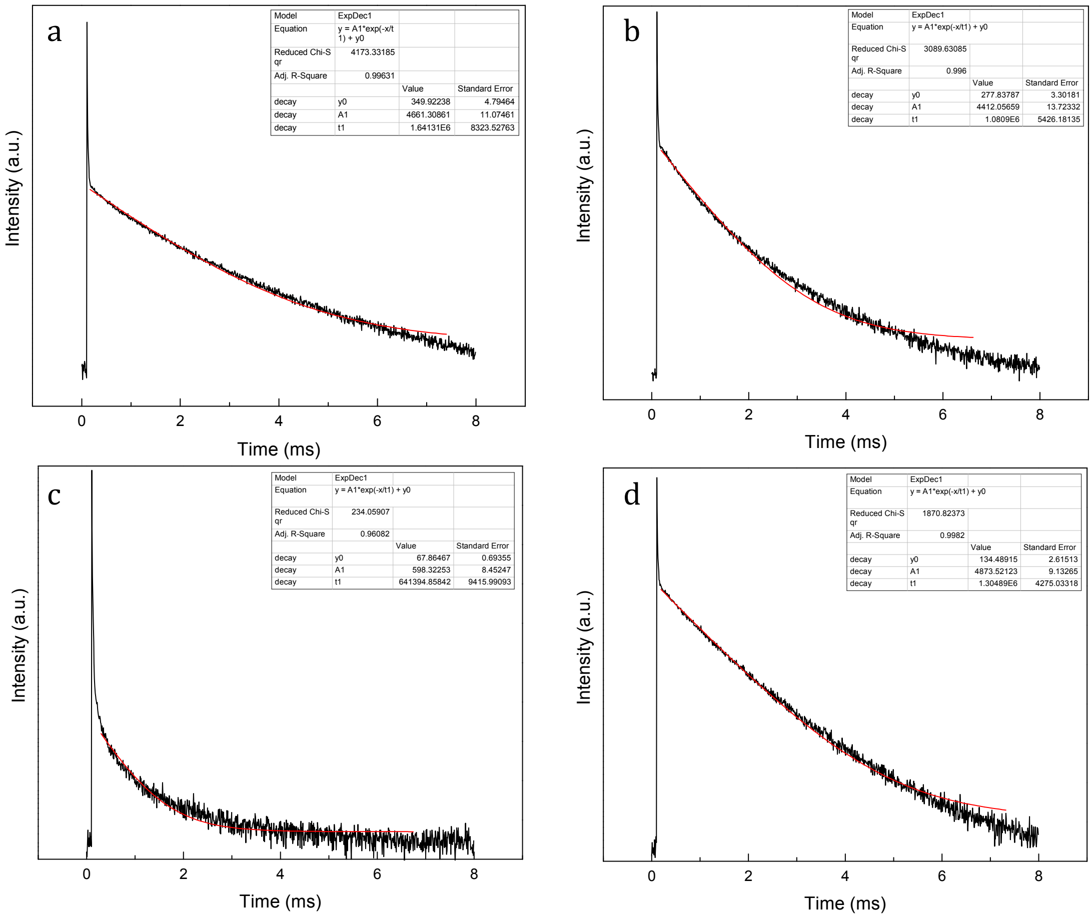

Fig. S14 Decay profiles for sample $Eu_{0.50}Tb_{0.50}$DPA-PMO a) 260 K observed at 544.6 nm (Tb), b) 260 K observed at 617.1 nm (Eu), c) 460 K observed at 544.6 nm (Tb), d) 460K observed at 617.1 nm (Eu). All decay times were recorded when exciting at 326.0 nm.

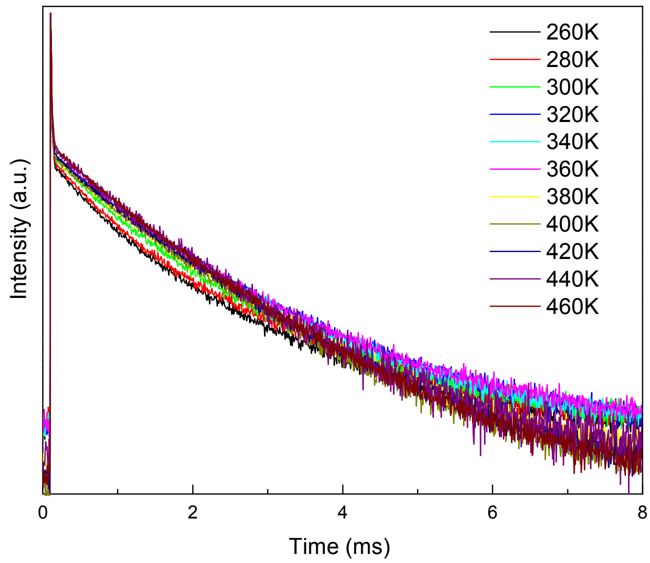

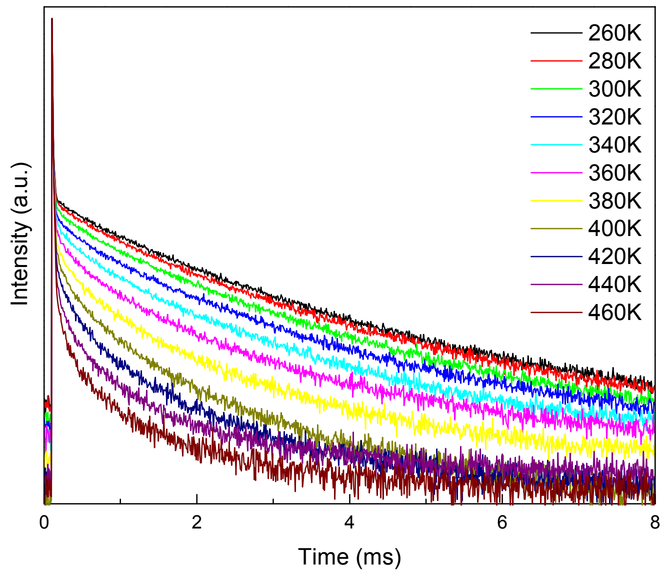

Fig. S15 Luminescence decay curves of (top) $^5D_0 \rightarrow {}^7F_2$ (617.1 nm, Eu^{3+}) and (bottom) $^5D_4 \rightarrow {}^7F_5$ (544.6 nm, Tb^{3+}) for $Eu_{0.50}Tb_{0.50}$DPA-PMO material recorded at different temperatures (the decay times were recorded when exciting at 326.0 nm.

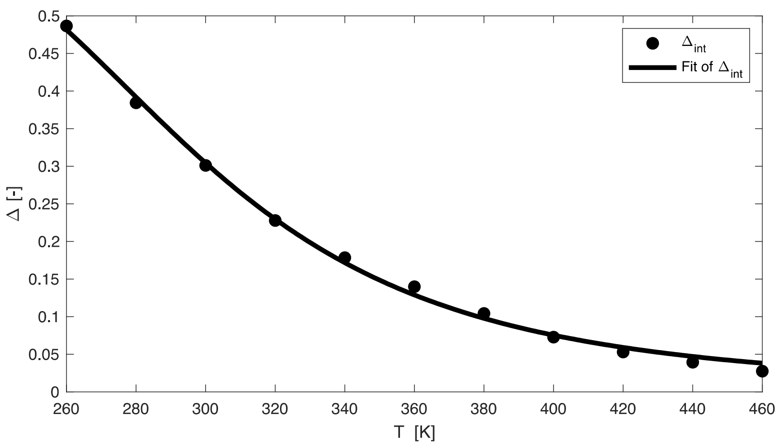

Fig. S16 Plot presenting the calibration curve for $Eu_{0.75}Tb_{0.25}$DPA-PMO material when eqn (2) is employed. The points show the experimental delta parameters and the solid line shows the best fit of the experimental points using eqn (2) (R^2 = 0.99774).

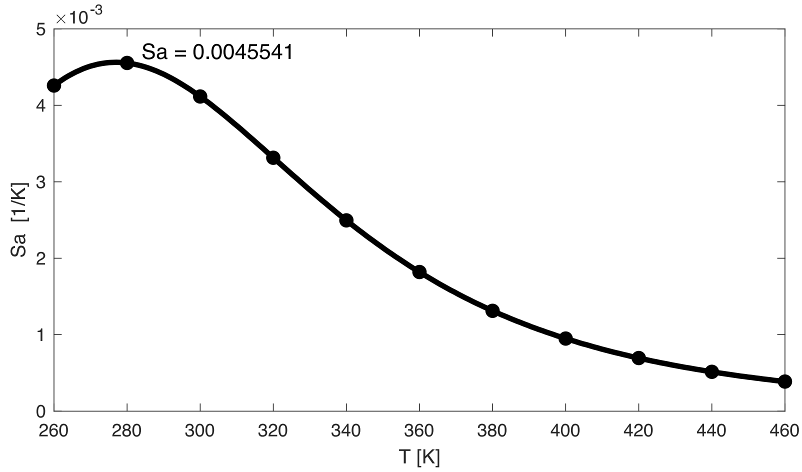

Fig. S17 Plot presenting the absolute sensitivity Sa values at varied temperatures (260K – 460K) for $Eu_{0.75}Tb_{0.25}$DPA-PMO. The solid lines are guides for eyes.

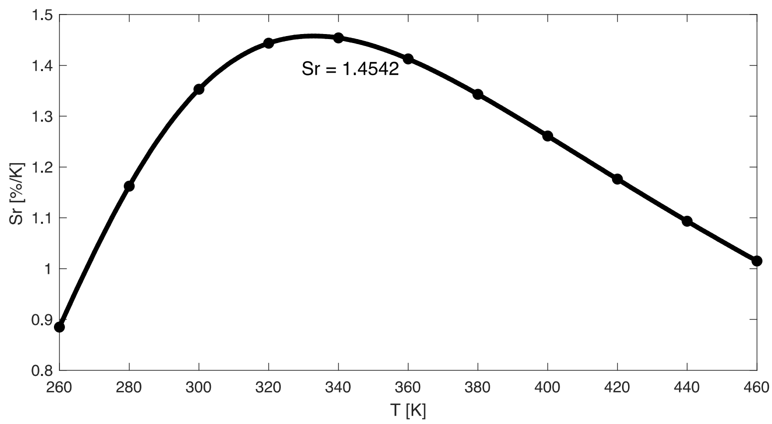

Fig. S18 Plot presenting the relative sensitivity Sr values at varied temperatures (260K – 460K) for compound $Eu_{0.75}Tb_{0.25}$DPA-PMO. The solid lines are guides for eyes.

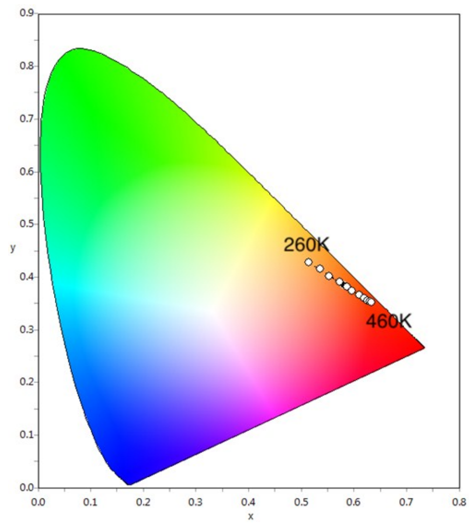

Fig. S19 CIE coordination diagram where the change of color for the $Eu_{0.75}Tb_{0.25}$DPA-PMO material is shown from 260 K to 460 K.

Table S7. CIE color coordinates (x, y) at different temperatures for $Eu_{0.75}Tb_{0.25}$DPA-PMO.

Temperature [K]	x coordinate	y coordinate
260	0.5151	0.4271
280	0.5360	0.4146
300	0.5535	0.4017
320	0.5736	0.3898
340	0.5872	0.3805
360	0.5968	0.3729
380	0.6100	0.3655
400	0.6193	0.3588
420	0.6262	0.3551
440	0.6312	0.3532
460	0.6331	0.3523

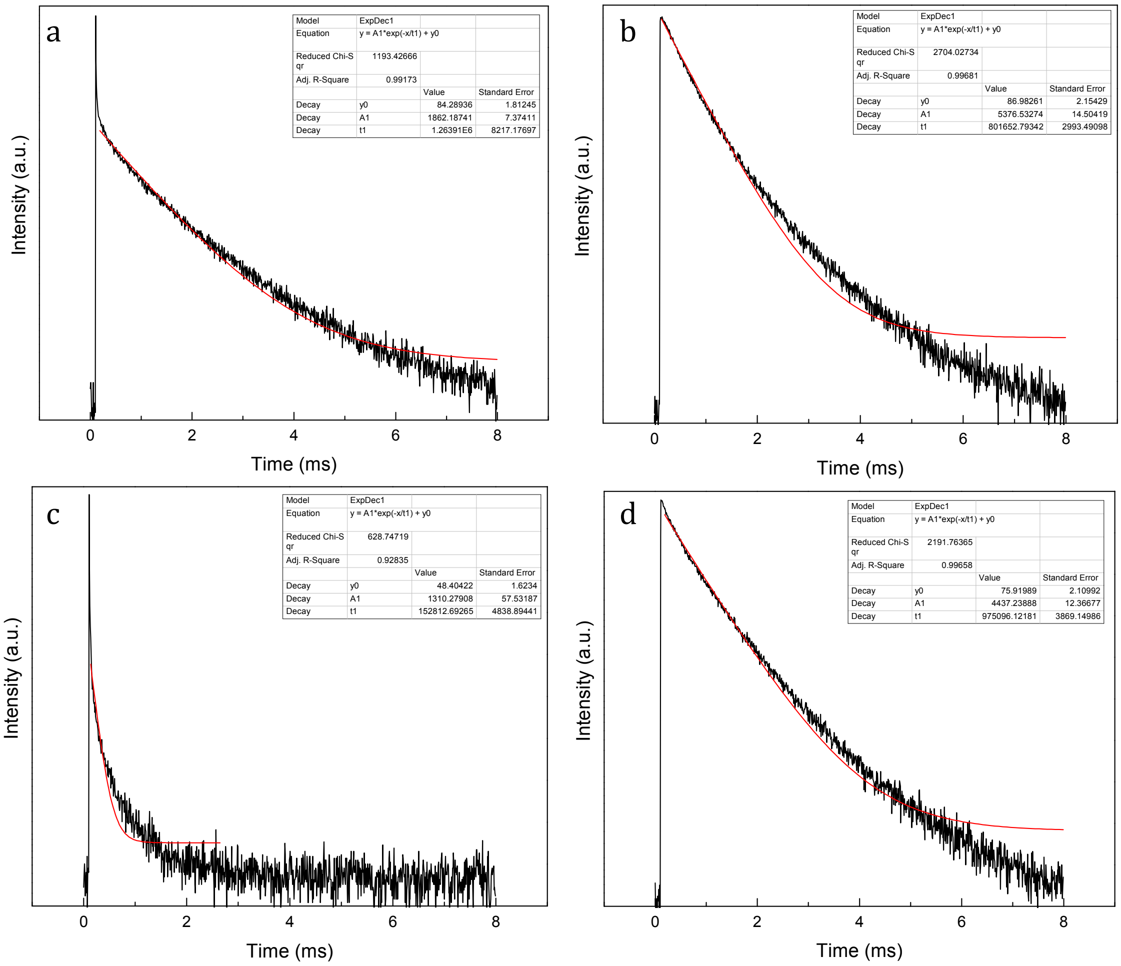

Fig. S20 Decay profiles for sample $Eu_{0.75}Tb_{0.25}$DPA-PMO a) 260 K observed at 544.0 nm (Tb), b) 260 K observed at 617.7 nm (Eu), c) 460 K observed at 544.0 nm (Tb), d) 460K observed at 617.7 nm (Eu). All decay times were recorded when exciting at 326.0 nm.

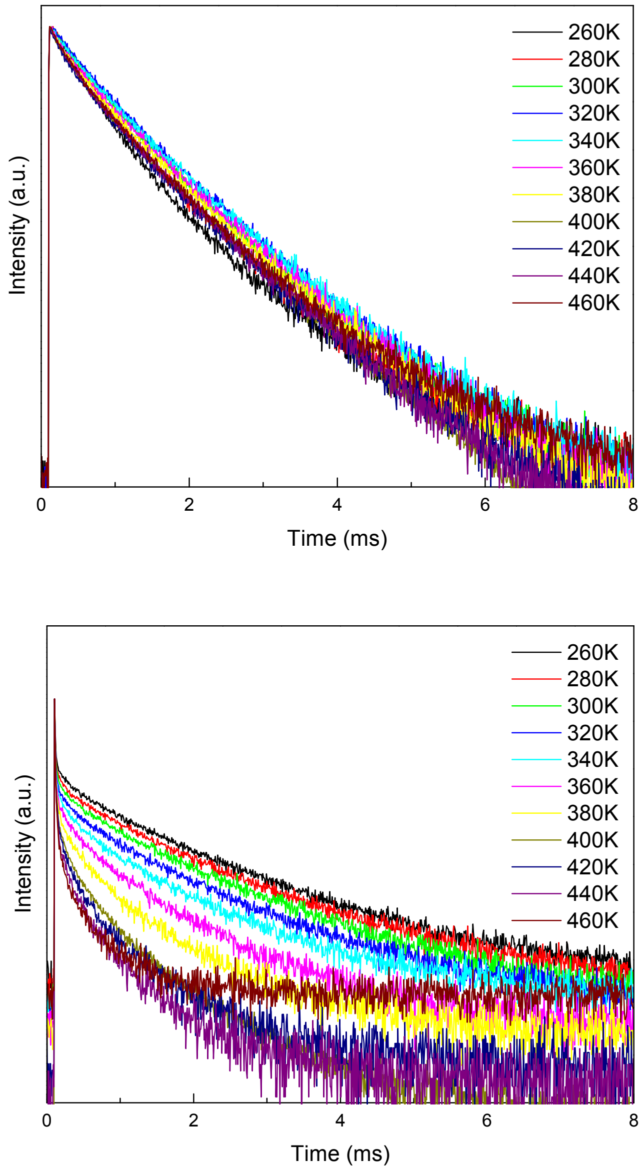

Fig. S21 Luminescence decay curves of (top) $^5D_0 \rightarrow {}^7F_2$ (617.7 nm, Eu^{3+}) and (bottom) $^5D_4 \rightarrow {}^7F_5$ (544.0 nm, Tb^{3+}) for $Eu_{0.75}Tb_{0.25}$DPA-PMO material recorded at different temperatures (the decay times were recorded when exciting at 326.0 nm

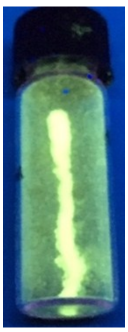

Fig. S22 Photo of $Sm_{0.90}Tb_{0.10}$DPA-PMO under 302 nm excitation under UV lamp.

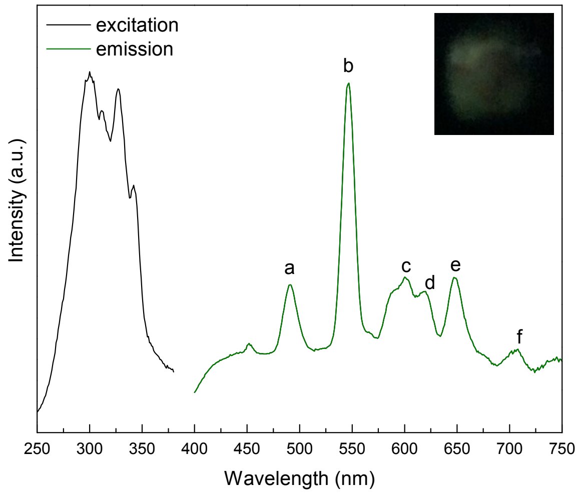

Fig. S23 Room temperature combined excitation-emission spectrum of sample $Sm_{0.95}Tb_{0.05}$DPA-PMO (excited a 326.0 nm and observed at 546.7 nm). The inset is a photo of the sample taken in the cryostat holder, excited at 326.0 nm with a xenon lamp.

Table S8. Assignment of peaks labeled in Fig. S23 ($Sm_{0.95}Tb_{0.05}$DPA-PMO).

Peak	Wavelength (nm)	Wavenumber (cm^{-1})	Transition
		Emission	
a	491.5	20346	$^5D_4 \rightarrow ^7F_6$ (Tb)
b	546.8	18288	$^5D_4 \rightarrow ^7F_5$ (Tb)
c	601.3	16633	$^5G_{5/2} \rightarrow ^6H_{7/2}$ (Sm)
d	619.3	16147	$^5D_4 \rightarrow ^7F_3$ (Tb)
e	647.8	15436	$^5G_{5/2} \rightarrow ^6H_{9/2}$ (Sm)
f	707.5	14134	$^5G_{5/2} \rightarrow ^6H_{11/2}$ (Sm)

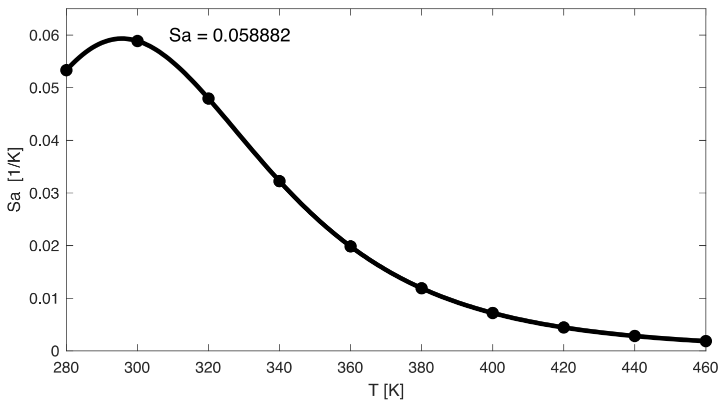

Fig. S24 Plot presenting the absolute sensitivity Sa values at varied temperatures (280K – 460K) for $Sm_{0.95}Tb_{0.05}$DPA-PMO. The solid lines are guides for eyes.

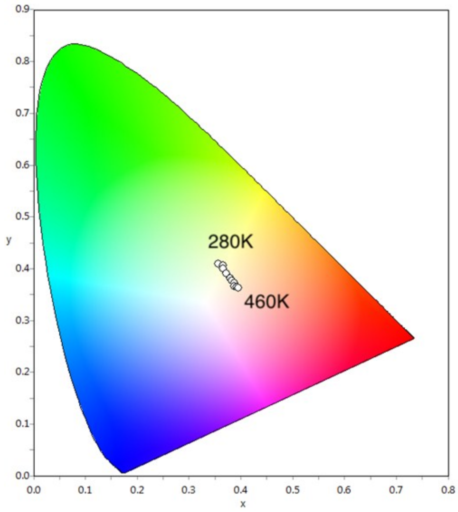

Fig. S25 CIE coordination diagram where the change of color for the $Sm_{0.95}Tb_{0.05}$DPA-PMO material is shown from 280 K to 460 K.

Table S9. CIE color coordinates (x, y) at different temperatures for $Sm_{0.95}Tb_{0.05}$DPA-PMO.

Temperature [K]	x coordinate	y coordinate
280	0.3565	0.4097
300	0.3655	0.4058
320	0.3664	0.3934
340	0.3721	0.3900
360	0.3795	0.3819
380	0.3832	0.3759
400	0.3881	0.3723
420	0.3883	0.3654
440	0.3918	0.3642
460	0.3961	0.3629

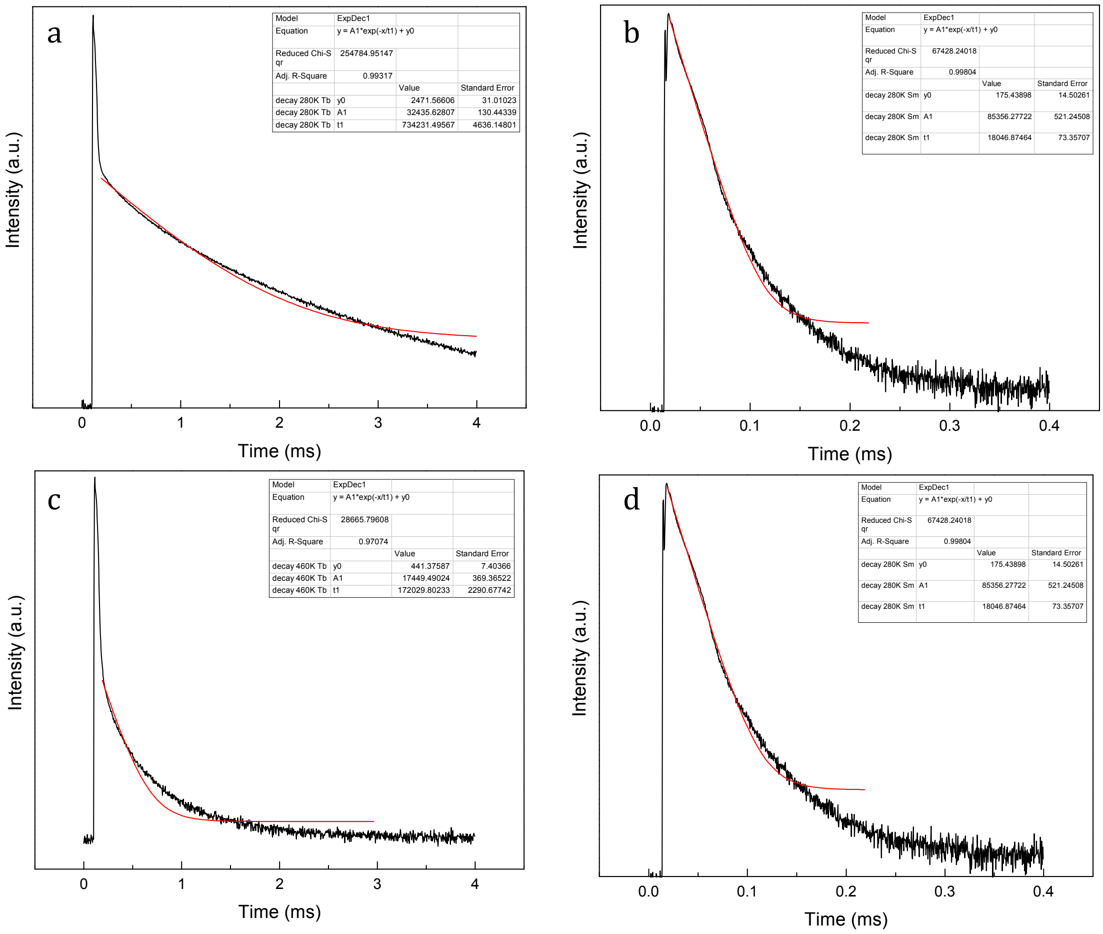

Fig. S26 Decay profiles for sample $Sm_{0.95}Tb_{0.05}$DPA-PMO a) 280 K observed at 546.8 nm (Tb), b) 280 K observed at 647.8 nm (Sm), c) 460 K observed at 546.8 nm (Tb), d) 460K observed at 647.8 nm (Sm). All decay times were recorded when exciting at 326.0 nm.

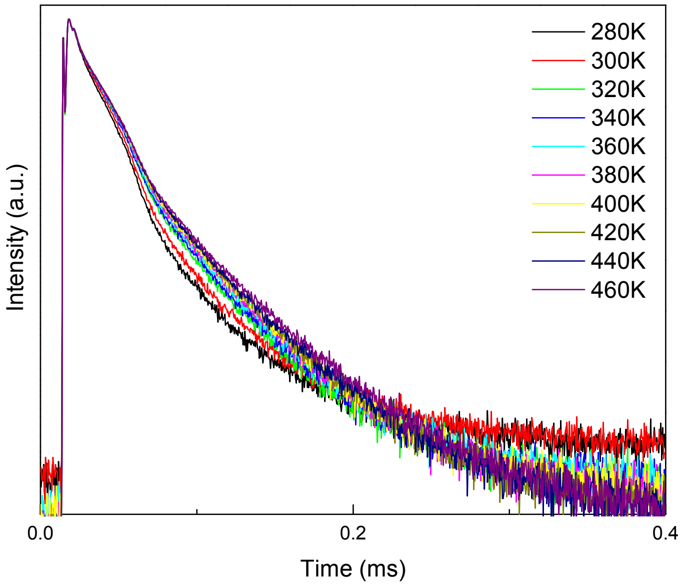

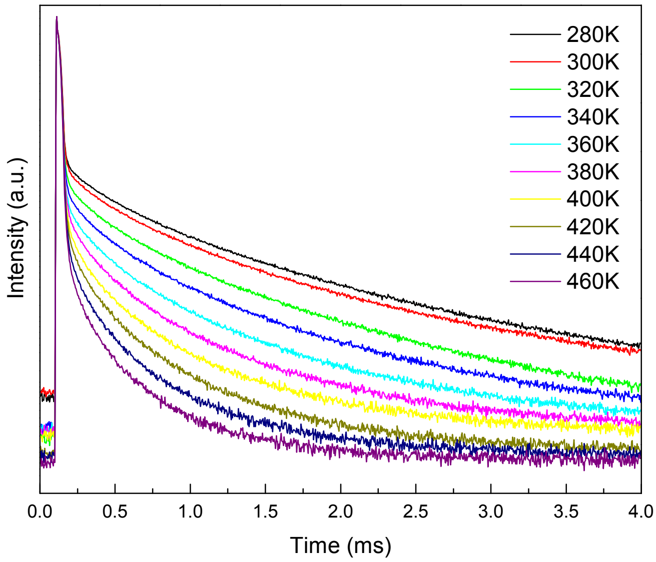

Fig. S27 Luminescence decay curves of (top) $^5G_{5/2}\rightarrow^6H_{9/2}$ (647.8 nm, Sm^{3+}) and (bottom) $^5D_4 \rightarrow {}^7F_5$ (546.8 nm, Tb^{3+}) for $Sm_{0.95}Tb_{0.05}$DPA-PMO material recorded at different temperatures (the decay times were recorded when exciting at 326.0 nm.

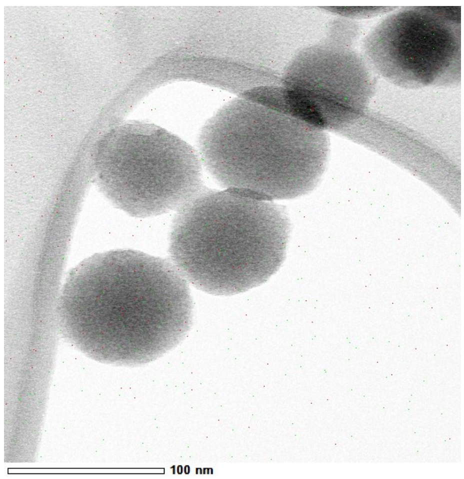

Fig. S28 TEM-EDX of $Eu_{0.50}Tb_{0.50}$DPA-PMO showing Eu/Tb grafted onto the PMO material.